ARTICLES

A mutation in Orai1 causes immune deficiency by abrogating CRAC channel function

Stefan Feske[1,2]*, Yousang Gwack[1,3]*, Murali Prakriya[4], Sonal Srikanth[1,3], Sven-Holger Puppel[1], Bogdan Tanasa[1], Patrick G. Hogan[1], Richard S. Lewis[5], Mark Daly[6,7] & Anjana Rao[1,3]

Antigen stimulation of immune cells triggers Ca^{2+} entry through Ca^{2+} release-activated Ca^{2+} (CRAC) channels, promoting the immune response to pathogens by activating the transcription factor NFAT. We have previously shown that cells from patients with one form of hereditary severe combined immune deficiency (SCID) syndrome are defective in store-operated Ca^{2+} entry and CRAC channel function. Here we identify the genetic defect in these patients, using a combination of two unbiased genome-wide approaches: a modified linkage analysis with single-nucleotide polymorphism arrays, and a *Drosophila* RNA interference screen designed to identify regulators of store-operated Ca^{2+} entry and NFAT nuclear import. Both approaches converged on a novel protein that we call Orai1, which contains four putative transmembrane segments. The SCID patients are homozygous for a single missense mutation in *ORAI1*, and expression of wild-type Orai1 in SCID T cells restores store-operated Ca^{2+} influx and the CRAC current (I_{CRAC}). We propose that Orai1 is an essential component or regulator of the CRAC channel complex.

Ca^{2+} is an essential second messenger in almost all cell types. Sustained Ca^{2+} influx across the plasma membrane is crucial for lymphocyte activation and the adaptive immune response[1–4]. Antigen recognition by T and B lymphocytes triggers phospholipase Cγ activation, inositol-1,4,5-triphosphate (IP_3) generation and the release of Ca^{2+} from endoplasmic reticulum (ER) stores. Depletion of ER Ca^{2+} stores opens CRAC channels, a class of 'store-operated' Ca^{2+} channels with high selectivity for Ca^{2+} over monovalent cations, low single-channel conductance (<1 pS) and an inwardly rectifying current–voltage (I–V) relationship[1,5–8]. One of the main Ca^{2+}-regulated transcription factors is NFAT, a family of heavily phosphorylated proteins that reside in the cytoplasm of resting cells[2,3]. Sustained Ca^{2+} influx results in NFAT dephosphorylation by the calmodulin-dependent protein phosphatase calcineurin and promotes NFAT translocation to the nucleus.

CRAC channels are a principal pathway for Ca^{2+} influx in T cells[1–4,9,10]. T cells from two patients with hereditary severe combined immune deficiency (SCID) syndrome, who presented as infants with a marked propensity for fungal and viral infections[11,12], had a primary defect in store-operated Ca^{2+} entry and CRAC channel function[9,13]. The SCID T cells also showed a severe impairment in NFAT-dependent gene activation[13–15], highlighting the importance of CRAC channel function for lymphocyte activation and immune defence.

Although the pharmacological and electrophysiological properties of the CRAC channel have been described in detail[1,5–7,16], its molecular identity is unknown. Several members of the transient receptor potential (TRP) family of ion channels have been proposed as candidates[17–20], but none of them has all the biophysical properties expected of the CRAC channel[7,8,21,22]. Sequence analyses and complementation studies in the SCID patients' cells[9] failed to establish a causative role for several TRP family members (TRPC3, TRPV5 and TRPV6) or for the EF-hand-containing membrane proteins STIM1 and STIM2, which couple store depletion to CRAC channel opening by sensing the filling state of ER Ca^{2+} stores[23–26].

Here we identify a novel protein, that we designate Orai1, which is crucial for store-operated Ca^{2+} entry and CRAC channel function. We identified Orai1 using two unbiased genetic approaches: a modified linkage analysis to identify the gene mutated in the SCID patients, and a genome-wide RNA interference (RNAi) screen in *Drosophila* to identify regulators of store-operated Ca^{2+} entry and NFAT nuclear import. The combination of these two approaches pinpointed a single candidate gene. RNAi-mediated depletion of *Drosophila Orai* (d*Orai*) markedly diminished store-operated Ca^{2+} entry; likewise, the Ca^{2+} influx defect in the SCID patients was traced to a point mutation in human *ORAI1*. Complementation of SCID T cells and fibroblasts with wild-type Orai1 reconstituted store-operated Ca^{2+} influx and the CRAC channel current (I_{CRAC}), establishing a critical role for Orai1 in T-cell function and the *in vivo* immune response. We propose that Orai1 is a subunit or key regulator of the CRAC channel complex.

Phenotypic identification of heterozygous disease carriers

The two SCID patients in our study were born to consanguineous parents, suggesting a recessive mode of inheritance as neither the patients' parents nor any other members of their extended family showed clinical symptoms of immunodeficiency (Fig. 1a). In the

[1]The CBR Institute for Biomedical Research, and the Departments of [2]Pediatrics and [3]Pathology, Harvard Medical School, 200 Longwood Avenue, Boston, Massachusetts 02115, USA. [4]Department of Molecular Pharmacology and Biological Chemistry, Northwestern University, Feinberg School of Medicine, Chicago, Illinois 60611, USA. [5]Department of Molecular and Cellular Physiology, Stanford University School of Medicine, Stanford, California 94305, USA. [6]Center for Human Genetic Research, Massachusetts General Hospital, Boston, Massachusetts 02114, USA. [7]Broad Institute of Harvard University and Massachusetts Institute of Technology, Cambridge, Massachusetts 02139, USA. *These authors contributed equally to this work.

presence of 2 mM extracellular Ca^{2+} ($[Ca^{2+}]_o$), T cells derived from the parents of the SCID patients showed almost normal store-operated Ca^{2+} entry[13]. To unmask a potential defect in Ca^{2+} entry in the parental T cells, we limited the driving force for Ca^{2+} entry by reducing $[Ca^{2+}]_o$ to 0.2–0.5 mM, and estimated the rate of Ca^{2+} influx indirectly by measuring the initial rate of change in intracellular Ca^{2+} concentration ($d[Ca^{2+}]_i/dt$) in cells treated with thapsigargin, an inhibitor of the SERCA Ca^{2+} pump. Under these conditions, peak $[Ca^{2+}]_i$ levels and initial rates of $[Ca^{2+}]_i$ increase in T cells from the parents were ~50% of those observed in wild-type control T cells (Fig. 1b). This finding is consistent with a gene-dosage effect, in which the parents are heterozygous carriers of the causal mutation for SCID.

We used this assay to identify, in a more extended pedigree, other potentially heterozygous carriers of the mutation responsible for the SCID phenotype. Blood samples were obtained from 19 additional family members (Fig. 1a), T-cell lines were generated, and Ca^{2+} entry measurements were made. T cells from 13 family members consistently showed reduced peak $[Ca^{2+}]_i$ levels and decreased initial rates of $[Ca^{2+}]_i$ increase, compared to cells from eight other family members and unrelated controls (Fig. 1c and data not shown). On the basis of these data, a cutoff value of $2\,nM\,s^{-1}$ for the rate of $[Ca^{2+}]_i$ increase was used to distinguish potential heterozygous disease carriers from unaffected individuals (Fig. 1c). With this cutoff, the distribution of putative heterozygous carriers within the family is compatible with an autosomal recessive mode of inheritance of the clinical disease (Fig. 1a).

Linkage mapping by genome-wide SNP array screen

Genomic DNA from the 23 members of the SCID family was used for genotyping using SNP mapping arrays. Data from the two patients, their parents, their unaffected brother and their grandparents were first evaluated assuming an autosomal recessive mode of inheritance based on the clinical phenotype (Pedigree A, grey shaded area in Fig. 1a). This analysis identified six regions with LOD ($\log_{10}$ of the odds ratio) scores of 1.5–1.9 (Fig. 2a, top panel). Although one of these regions is almost certain to harbour the defective gene, the LOD scores are significantly below the 3.0 value necessary to establish linkage, and so might be achieved by chance. We therefore implemented a second, completely independent analysis in which we assumed an autosomal dominant mode of inheritance, based on our ability to identify heterozygous carriers of the disease mutation by phenotypic analysis in vitro (Pedigree B, green box in Fig. 1a). The haplotype of twelve putatively heterozygous individuals was compared to that of the remaining eight homozygous healthy family members, identifying a unique region on chromosome 12q24 with a LOD score of ~3.8, which overlapped with one of the six regions identified by the first approach (Fig. 2a, middle panel). This defines a ~9.8-Mb candidate region with a highly significant cumulative LOD score of 5.7, representing odds of ~500,000:1 in favour of linkage (Fig. 2a, bottom panel and Fig. 2b). Genomic sequencing of six known genes in this region with a potential role in Ca^{2+} signalling or Ca^{2+} binding (PLA2G1B, CABP1, P2RX4, P2RX7, CAMKK2 and PITPNM2) did not reveal any mutations in exons or immediately adjacent genomic regions, but did allow us to narrow down the candidate homozygous region to ~6.5 Mb containing ~74 genes, on the basis of several SNPs in PITPNM2 for which the patients were heterozygous (Fig. 2c).

Drosophila olf186-F is a regulator of Ca^{2+} entry

In parallel with the positional cloning effort, we conducted a genome-wide RNAi screen[27,28] for NFAT regulators in Drosophila, as an independent method of identifying components of the CRAC channel and the signalling pathway leading to CRAC channel activation. This screen takes advantage of the fact that although Ca^{2+}-regulated NFAT proteins are not represented in Drosophila, there is strong evolutionary conservation of the pathways that regulate NFAT shuttling between the cytoplasm and nucleus[29]. For example, Drosophila S2 cells contain a store-operated Ca^{2+} channel that is very similar to the CRAC channel[30]. Drosophila S2R+ cells stably expressing an NFAT–green fluorescent protein (GFP) fusion protein were incubated for four days with arrayed double-stranded (ds)RNAs against each of ~21,000 Drosophila genes to achieve knockdown of gene expression[29]. The cells were stimulated for 10 min with thapsigargin to deplete Ca^{2+} stores, thus activating store-operated Ca^{2+} entry and nuclear translocation of NFAT–GFP, then fixed and photographed robotically.
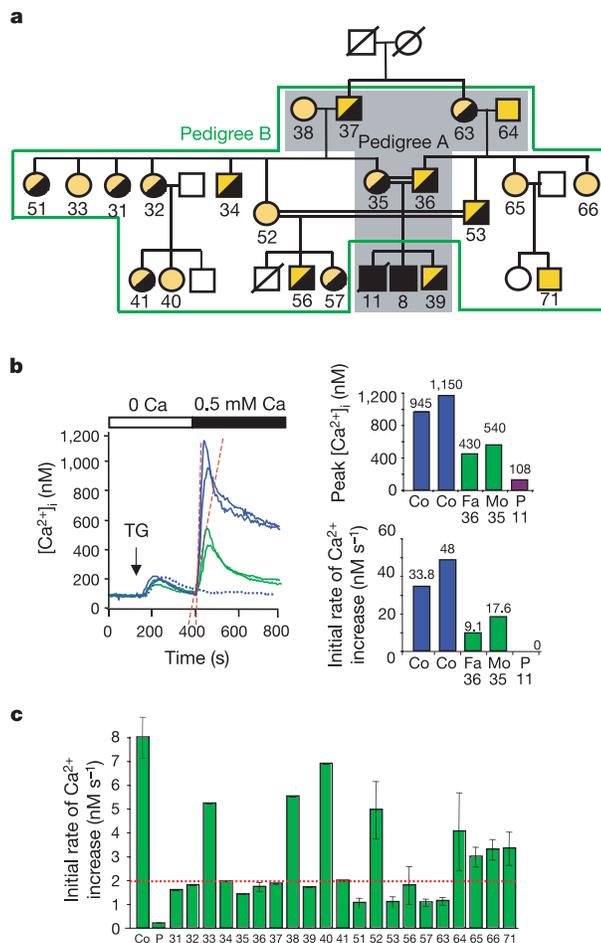

Figure 1 | Gene-dosage effect in store-operated Ca^{2+} entry. a, Pedigree of SCID patients with a defect in store-operated Ca^{2+} entry. Black boxes indicate patients with SCID (individuals 8 and 11), diagonal bars indicate deceased individuals, symbols consisting of two different colours indicate heterozygous disease carriers as determined by phenotypic analysis, and double horizontal bars indicate consanguineous marriages. DNA and lymphocytes were obtained for functional and genetic analysis from all individuals to whom a number is assigned. **b**, Reduced Ca^{2+} influx in T cells of both parents of the SCID patients (green) compared to wild-type controls (blue). Peak $[Ca^{2+}]_i$ (top right panel) and initial rates of $[Ca^{2+}]_i$ increase (bottom right panel) were measured in thapsigargin (TG)-stimulated T cells after re-addition of 0.5 mM extracellular Ca^{2+}. Dashed red lines indicate initial slopes of $[Ca^{2+}]_i$ increase. The dashed blue trace represents the Ca^{2+} response in T cells from SCID patients. **c**, Reduced store-operated Ca^{2+} entry in T cells from 13 out of 21 family members of the SCID patients identifies them as heterozygous disease carriers. Shown are averages of the initial rates of $[Ca^{2+}]_i$ influx in the presence of 0.2 mM $[Ca^{2+}]_o$. Identification numbers correspond to individuals shown in **a**. Stars indicate heterozygous carriers with initial rates of Ca^{2+} influx less than or equal to $2\,nM\,s^{-1}$ (dotted red line). Co, healthy control; P, SCID patient; Fa, father; Mo, mother. Error bars represent s.e.m. from three independent experiments (50–100 cells analysed per experiment).

Among the positive candidates for which depletion interfered with nuclear translocation and dephosphorylation of NFAT–GFP were *Drosophila Stim* (d*Stim*) and *olf186-F* (hereafter designated d*Orai*, for reasons discussed below) (Fig. 3a, b). Knockdown of either d*Stim* or d*Orai* completely inhibited thapsigargin-induced Ca^{2+} influx in S2R+ cells (Fig. 3c), but had no effect on the filling state of Ca^{2+} stores (Supplementary Fig. 1). These data confirm previous reports that dSTIM is essential for activation of store-operated Ca^{2+} entry and of a CRAC channel-like current in *Drosophila* cells[24], and identify dOrai as a second regulator of this process.

olf186-F has three human homologues, *FLJ14466* on chromosome 12, *C7orf19* on chromosome 7 and *MGC13024* on chromosome 16.

Notably, *FLJ14466* is located within the 6.5-Mb homozygous genomic region linked to the SCID mutation at 12q24 (Fig. 2c), and contains the causal mutation for the SCID syndrome as shown below. We have named the proteins encoded by *FLJ14466*, *C7orf19* and *MGC13024* as Orai1, Orai2 and Orai3, respectively. (In Greek mythology, the Orai are the keepers of the gates of heaven: Eunomia (Order or Harmony), Dike (Justice) and Eirene (Peace)[31,32].)

ORAI1 is mutated in the SCID patients

By sequencing genomic DNA from the 23 individuals (patients and their relatives) indicated in Fig. 1a, we found that the SCID defect is associated with a missense mutation in exon 1 of human *ORAI1* (Fig. 4a). The mutation is a C→T transition at position 271 of the coding sequence of *ORAI1* (position 444 of NM_032790), leading to replacement of a highly conserved arginine residue by tryptophan at position 91 of the protein (R91W) (Supplementary Fig. 2). All 13 phenotypically predicted heterozygous disease carriers (Fig. 1) were genotypically heterozygous for the mutation (C/T), whereas healthy controls and unaffected family members were homozygous for the wild-type allele (C/C) (Fig. 4a and data not shown).
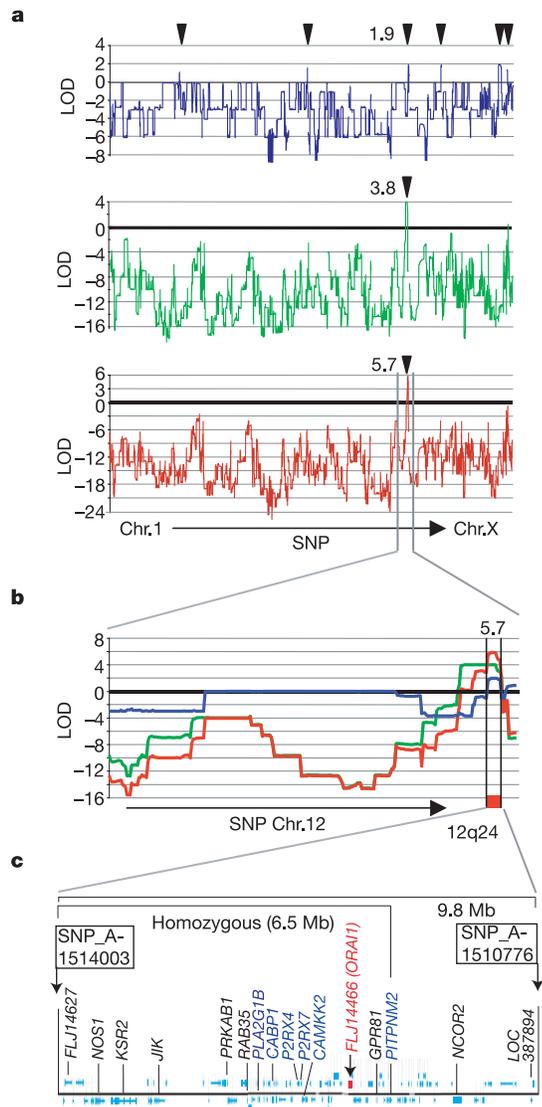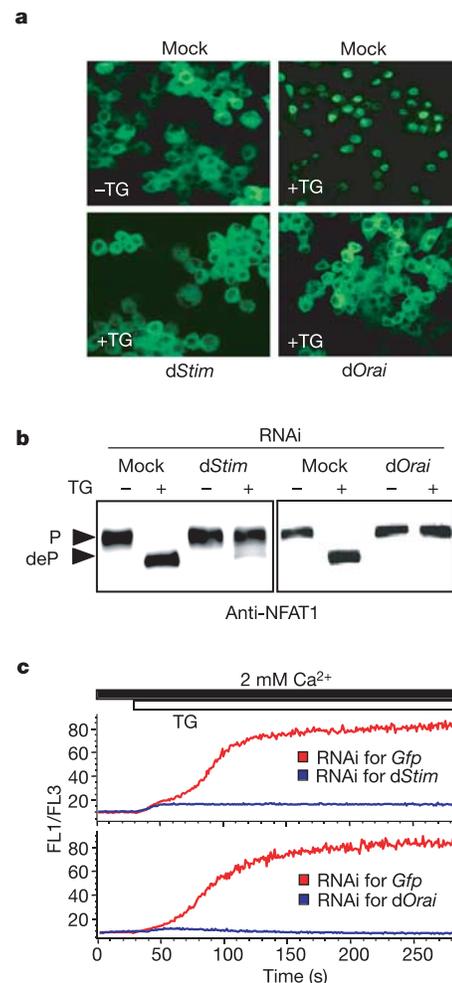

Figure 2 | A region on chromosome 12q24 is linked to the SCID gene defect. Genome-wide linkage analysis in 23 individuals from the SCID family. **a,** Multipoint parametric LOD scores were calculated for >10,000 SNPs. LOD scores derived from autosomal recessive (top) and dominant (middle) analyses were combined to yield a 'cumulative' LOD score (bottom) and plotted against the position of SNP markers in the genome (horizontal axis). Arrows indicate regions statistically linked to the SCID disease. **b**, A unique candidate gene region on 12q24 shows a highly significant cumulative LOD score (red trace) of 5.7. **c**, The ~6.5-Mb genomic interval on 12q24 contains *FLJ14466* (*ORAI1*). Genes sequenced in the SCID patients are shown in blue, other genes in black. The graphic representation of the candidate region was modified from NCBI MapViewer (http://www.ncbi.nlm.nih.gov/mapview/).

Figure 3 | *Drosophila* Orai regulates NFAT translocation and Ca^{2+} influx. S2R+ cells stably transfected with GFP–NFAT1(1–460) were incubated for four days with dsRNA against d*Stim*, d*Orai* or an irrelevant DNA sequence (mock). **a, b,** Knockdown of d*Orai* or d*Stim* prevents thapsigargin-induced nuclear translocation (**a**) and dephosphorylation (deP) (**b**) of NFAT–GFP. **c,** RNAi-mediated depletion of d*Stim* or d*Orai* inhibits Ca^{2+} influx in S2R+ cells. Cells were loaded with Fluo-4 and Fura-Red and analysed for Ca^{2+} influx by flow cytometry after stimulation with thapsigargin (1 µM). Traces show changes in the emission ratio of the Ca^{2+} indicator dyes Fluo-4 (FL1) and Fura Red (FL3).

The C→T mutation is not an annotated SNP (in dbSNP Build 124), nor is it represented in the DNA from 270 individuals of mixed ethnic backgrounds assembled for the international HapMap project[33] (data not shown), suggesting that it is not a common sequence variant in the general population. The mutated residue is located at the beginning of the first of four potential transmembrane segments in Orai1, predicted by calculating the hydrophobicity of Orai1 using the Kyte–Doolittle method[34] (Fig. 4b). We showed that Orai1 is localized at or near the plasma membrane by expressing amino- or carboxy-terminal Myc-tagged Orai1 in SCID cells using a bicistronic IRES–GFP retroviral vector (Fig. 4d). Non-permeabilized cells did not stain with an anti-Myc antibody (unpub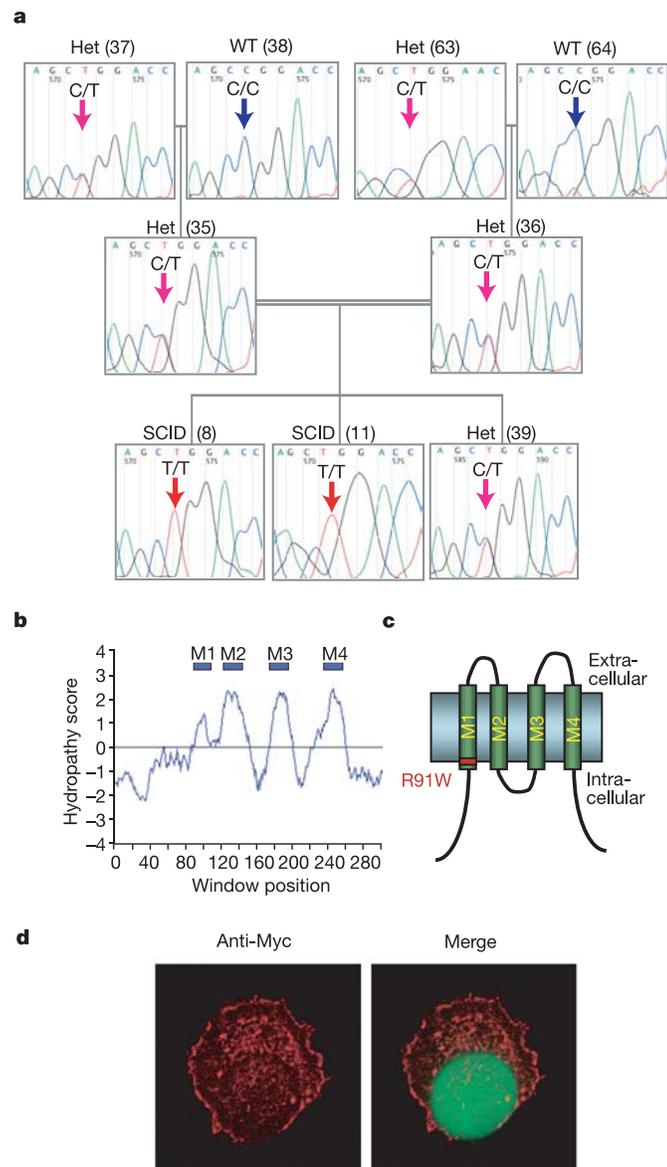lished data), consistent with a topology in which both the N and C termini are cytoplasmically oriented and so inaccessible to the antibody (Fig. 4c).

Orai1 restores store-operated Ca^{2+} influx in the SCID T cells

Expression of wild-type Orai1 (Orai1(WT)) complements the Ca^{2+} influx defect in SCID T cells and fibroblasts, but mutant R91W Orai1 (Myc–Orai1(R91W)) does not (Fig. 5a–d and Supplementary Fig. 3). Myc-tagged Orai1(WT) expressed in SCID cells using an IRES–GFP retroviral vector restored thapsigargin-induced Ca^{2+} influx in GFP-positive but not GFP-negative cells (Fig. 5 and Supplementary Fig. 3). Notably, Ca^{2+} influx was observed only after store depletion with thapsigargin even when $[Ca^{2+}]_o$ was increased to 20 mM (Supplementary Fig. 3g). This behaviour is a defining feature of store-operated Ca^{2+} entry through CRAC channels, and shows that Orai1 does not encode a constitutively open Ca^{2+} channel.

Mutant and wild-type Orai1 were expressed at equivalent levels and showed similar localization at and near the plasma membrane, as judged by immunocytochemistry (Fig. 4d and Supplementary Fig. 4) and western blotting (data not shown). The pharmacological
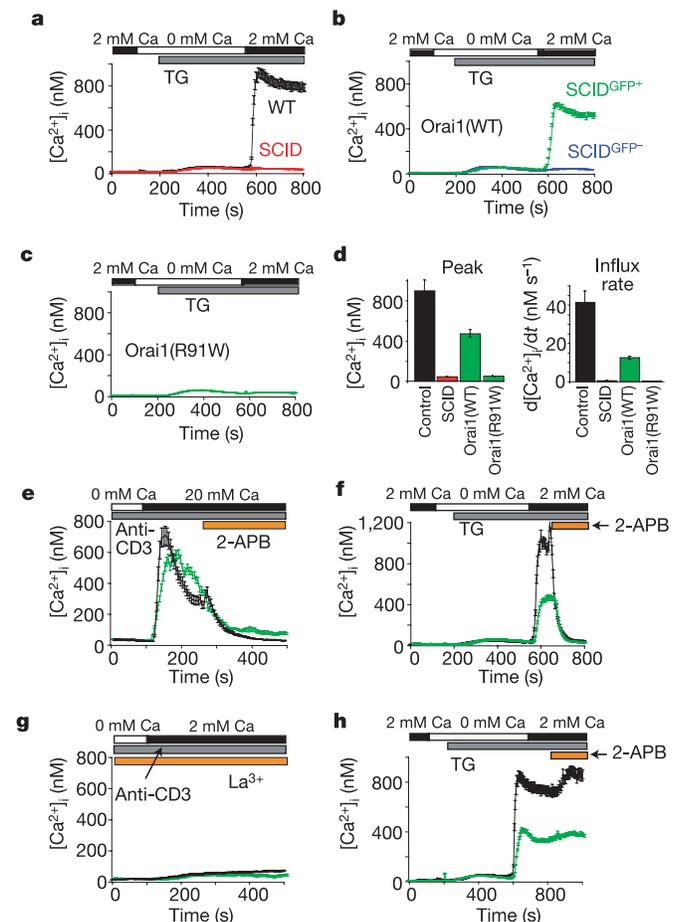

Figure 4 | ORAI1 is mutated in the SCID patients. a, Homozygous C→T missense mutation in both SCID patients (8, 11). Other family members (parents, grandparents and unaffected brother) are heterozygous (Het) or wild type (WT) at this position. Identification numbers of individuals as in Fig. 1a. **b**, Hydropathy plot of Orai1 calculated using the Kyte–Doolittle algorithm, with a window size of 19 amino acids. Three transmembrane segments (M2–M4) are predicted to have a score >1.8; M1 has a lower score of ~1.3. **c**, Schematic representation of the predicted membrane topology of Orai1. **d**, Myc-tagged Orai1(WT) (red), coexpressed with GFP (green) in SCID T cells, localizes at or near the plasma membrane.

Figure 5 | Orai1 complements the Ca^{2+} entry defect in SCID patients' T cells. a, Ca^{2+} influx in untransduced T cells from a control (black) and a SCID patient (red). **b, c**, Expression of wild-type Myc–Orai1(WT) (green trace in **b**), but not mutant Myc–Orai1(R91W) (green trace in **c**), in SCID T cells restores store-operated Ca^{2+} entry. **d**, Summary of peak $[Ca^{2+}]_i$ levels and initial rates of $[Ca^{2+}]_i$ increase compiled from several experiments similar to those shown in **a–c**. Averages were calculated from all GFP+ SCID T cells expressing Orai1(WT) and Orai1(R91W). Error bars represent s.e.m. from three independent experiments (50–100 cells analysed per experiment). **e–h**, Ca^{2+} influx in control T cells (black) and Myc–Orai1(WT)-expressing SCID T cells (green) is inhibited by 75 μM 2-APB (**e, f**) or 2 μM La^{3+} (**g**), and enhanced by 3 μM 2-APB (**h**) after stimulation with an anti-CD3 antibody (**e, g**) or thapsigargin (**f, h**).

characteristics of store-operated Ca^{2+} entry in Orai1-complemented cells were exactly those expected for Ca^{2+} influx through CRAC channels[7,35]. Treatment with $75\,\mu M$ 2-aminoethyldiphenyl borate (2-APB, a compound known to modulate CRAC channel activity) or $2\,\mu M$ La^{3+} inhibited Ca^{2+} influx, whereas treatment with a low dose of 2-APB ($3\,\mu M$) caused a distinct further increase in $[Ca^{2+}]_i$ (Fig. 5e–h and Supplementary Fig. 3). Together, these results show that *ORAI1* is the gene responsible for the Ca^{2+} influx defect in the T cells and fibroblasts of SCID patients.

Expression of Orai1 restores I_{CRAC} in the SCID T cells

Using a whole-cell patch-clamp configuration, we showed that the currents arising from store-depletion in reconstituted SCID T cells have many key features of I_{CRAC} (Fig. 6 and Supplementary Fig. 5).
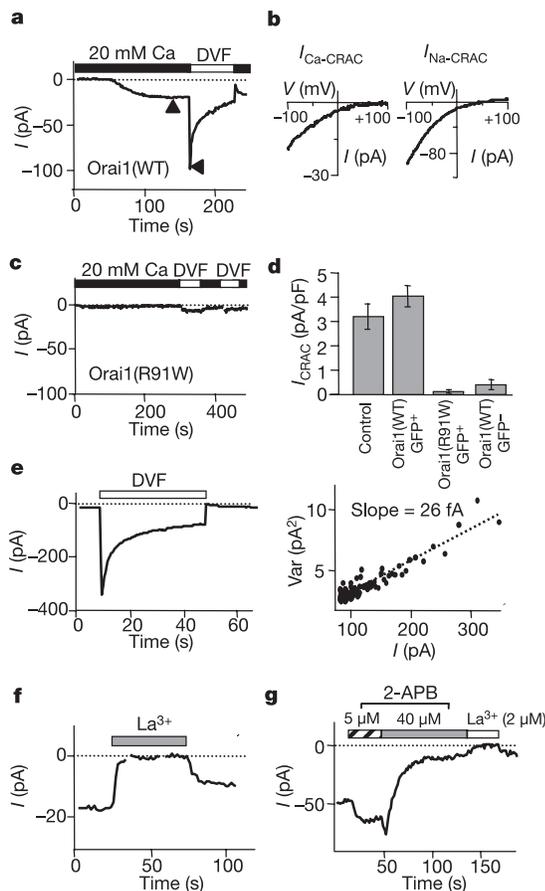

Figure 6 | Expression of Orai1 restores CRAC channel function in SCID T cells. a, Ca^{2+} and Na^+ CRAC currents in an Orai(WT)-complemented SCID T cell after passive store depletion with a pipette solution containing 8 mM BAPTA. **b,** Current–voltage (*I*–*V*) relationship in 20 mM $[Ca^{2+}]_o$ (left) and in divalent-free solution (DVF, right), collected at the times indicated by the arrows in **a. c,** In SCID T cells expressing mutant Orai1(R91W), Ca^{2+} and Na^+ currents fail to develop during passive store depletion by 8 mM BAPTA. **d,** Summary of peak current densities in the indicated cell categories. Cell numbers: control ($n = 5$), Orai1(WT) GFP$^+$ ($n = 10$), Orai1(R91W) GFP$^+$ ($n = 5$), Orai1(WT) GFP$^-$ ($n = 4$). Error bars represent s.e.m. **e,** Noise analysis of the depotentiating Na^+ current measured at a constant potential of -100 mV. Left plot shows the mean current; right plot shows the variance (Var) plotted against the mean current. **f,** Blockade of the Ca^{2+} current by $2\,\mu M$ La^{3+}. **g,** Potentiation and blockade of I_{CRAC} by low ($5\,\mu M$) and high ($40\,\mu M$) doses of 2-APB. Results are representative of 5 out of 5 cells. Panels **a, c, f** and **g** show peak currents elicited by hyperpolarizing steps to -100 mV. The leak-corrected zero current level is indicated by a dotted line (**a, c, e, f, g**). Cells expressing high GFP and Orai1(WT) or Orai1(R91W) were selected for patch-clamp recordings.

In SCID T cells reconstituted with wild-type but not mutant Myc–Orai1, inclusion of 8 mM BAPTA (a Ca^{2+} chelator) in the patch pipette caused slow development of an inward current in 20 mM $[Ca^{2+}]_o$, reminiscent of the development of I_{CRAC} in response to store depletion with BAPTA or thapsigargin[5,6] (Fig. 6a). In divalent-free solution lacking Ca^{2+} and Mg^{2+}, an inward Na^+ current was observed that was initially much larger than the Ca^{2+} current but subsequently declined over tens of seconds (Fig. 6a). This phenomenon, known as depotentiation, is characteristic of CRAC channels in Jurkat T cells, rat basophilic leukaemia (RBL) cells and human T-cell lines[9,16,36].

Both the Ca^{2+} and Na^+ currents showed an inwardly rectifying current–voltage (*I*–*V*) relationship (Fig. 6b). The reversal potential of the inward current in 20 mM Ca^{2+} was greater than $+90$ mV, consistent with the known high selectivity of CRAC channels for Ca^{2+}. The reversal potential in divalent-free solution was 49 ± 2 mV ($n = 4$ cells), indicating that, as expected[16,37], the channels are only weakly permeable to the Cs^+ ions in the patch pipette ($P_{Cs}/P_{Na} = 0.14$). The noise characteristics of the current were consistent with those of CRAC channels (Fig. 6e): during depotentiation of the Na^+ current, variance declined linearly with mean current, with an average slope of 29 ± 4 fA ($n = 4$ cells), providing a lower boundary for the unitary current similar to that of previous measurements of I_{CRAC}[16]. The Ca^{2+} current showed fast inactivation in 20 mM $[Ca^{2+}]_o$, and the extent and time course of inactivation was similar to that previously reported for CRAC channels in Jurkat T cells[38] (Supplementary Fig. 5d). The pharmacological hallmarks of the reconstituted current included complete block by $2\,\mu M$ La^{3+} (Fig. 6f), as well as potentiation by low doses and inhibition by high doses of 2-APB (Fig. 6g). Moreover, the block observed with high doses of 2-APB was accompanied by the loss of fast inactivation[35] (data not shown). Together, these studies show that a single point mutation in *ORAI1* disrupts CRAC channel function in T cells.

Discussion

We have used two independent genetic analyses to identify Orai1 as an evolutionarily conserved and essential component of the store-operated Ca^{2+} entry mechanism. Genome-wide SNP analysis of SCID patients and their relatives, analysed using a powerful combination of recessive and dominant linkage mapping, pinpointed a genomic region with a very high probability of linkage to the mutant gene. A parallel genome-wide screen in *Drosophila* identified several candidates for which RNAi-mediated depletion interfered with thapsigargin-mediated nuclear localization of NFAT–GFP. These candidates included d*Stim*, a known ER Ca^{2+} sensor and regulator of store-operated Ca^{2+} entry[24–26], and a novel candidate, *olf186-F* (here renamed *Drosophila Orai*). Validating our dual strategy, the gene encoding one of the human homologues of dOrai, Orai1 (hypothetical protein FLJ14466), is located on chromosome 12q24, exactly the region identified through our SNP analysis as genetically linked to the SCID syndrome. Additional studies confirmed that a point mutation in *ORAI1* is responsible for the genetic defect in store-operated Ca^{2+} entry and I_{CRAC} in cells of the SCID patients[9,13]. It will be interesting to determine whether *ORAI1* is also mutated in two other SCID patients identified as having similar defects in CRAC channel function[10,39], or whether these patients have defects in some other component of the signalling pathway leading to CRAC channel activation.

The genetic basis for the SCID defect is not a known polymorphism, nor is it represented in the 270 individuals of the HapMap panel[33], a number sufficient to find almost all haplotypes with frequencies $\geq 5\%$. The possibility that the C→T mutation is a single-nucleotide polymorphism confined to a small ethnic population not represented in the HapMap panel can be ruled out with reasonable certainty, based on the fact that complementation with Orai1 restores store-operated Ca^{2+} entry and I_{CRAC} in SCID patient

cells. Furthermore, arginine 91, which is mutated in the SCID patients, is located in a putative transmembrane region that is conserved across species (Fig. 4b, c and Supplementary Fig. 2), highlighting its potential importance in Orai1 function.

ORAI1 mRNA is broadly expressed in mammalian tissues (data not shown), potentially explaining previous observations that not only the T cells from SCID patients, but also B cells and fibroblasts, have a substantial defect in store-operated Ca^{2+} entry[13]. Surprisingly, however, the clinical phenotype of the SCID patients is predominantly one of immunodeficiency, associated in the single surviving patient with ectodermal dysplasia and anhydrosis (EDA) and a congenital, non-progressive myopathy (unpublished observations). EDA is characterized by defects in the morphogenesis of ectodermal structures, including hair, skin, sweat glands and teeth, and previous studies have linked it to hypoactivation of the transcription factor NF-κB[40–43]. Ca^{2+} mobilization is thought to contribute to NF-κB activation in T cells and other cell types under certain stimulatory conditions[44], thus the EDA syndrome may reflect defective NF-κB activation, either during development or acutely in specific cell types. In contrast, the myopathy could potentially be a direct consequence of defective NFAT activation, given that NFAT has a substantial influence on certain aspects of skeletal muscle development and function (reviewed in refs 3, 45).

The characteristics of Ca^{2+} influx and the Ca^{2+} current in Orai1-complemented SCID T cells are indistinguishable from those observed in control T cells. Both are strictly regulated by store depletion, and the electrophysiological and pharmacological properties of the restored current are fully consistent with those of I_{CRAC}. Although the specific role of Orai1 has not yet been determined, the available data are consistent with the possibility that Orai1 encodes a channel subunit or a closely associated channel regulator in the plasma membrane. The hydropathy profile of Orai1 predicts a membrane protein with four transmembrane segments (Fig. 4b, c). Immunocytochemistry of Myc-tagged Orai1 in resting cells is consistent with localization at the plasma membrane (Fig. 4d), and both N- and C-terminal epitope tags on Orai1 are inaccessible to antibody staining in non-permeabilized cells (data not shown), compatible with the topology of a plasma membrane channel subunit in which both N and C termini are cytoplasmic (Fig. 4c). The plasma membrane localization of Orai1 differs from that of STIM1, which is predominantly located in the ER[9,25,26]. Future studies will address the relation between Orai and Stim proteins and the mechanism by which store depletion couples to CRAC channel opening.

METHODS

The *Drosophila* genome-wide RNAi screen was performed as previously described[27–29]. Detailed descriptions of all methods are provided in the online Supplementary Information.

Single-nucleotide polymorphism array-based linkage analysis. Genomic DNA of SCID patients and 21 relatives was prepared from peripheral blood mononuclear cells using genomic DNA maxi prep kits (Qiagen). Genotyping was performed at the SNP Genotyping Center of the Broad Institute and the Harvard Partners Center for Genetics and Genomics, using Affymetrix Human Mapping 10K (Xba 142 2.0) microarrays with an average SNP heterozygosity of 0.38 and a mean intermarker distance of 258 kb, allowing for simultaneous genotyping of more than 10,000 SNPs in the human genome.

For parametric linkage analysis, data were converted into 'Linkage' format using 'Compare Linkage'[46], and imported into the multi-point linkage software programs Merlin and Allegro. Mendelian genotype errors inconsistent with the parental genotypes were detected and set to missing genotypes. Multipoint parametric linkage analysis was performed to compute LOD scores at each SNP position using Allegro[47], as shown in Fig. 2. Linkage analysis using Genehunter 2.1r6 provided very similar results. For parametric analysis, a disease allele frequency of 0.001, a penetrance value of 0.99 and a phenocopy of 0.01 were used for all of the pedigrees. Two distinct parametric linkage analyses were carried out using recessive and dominant models of inheritance, respectively. For the 'recessive' model, haplotypes from both patients, their parents, unaffected brother and grandparents (individuals 8, 11, 35, 36, 37, 38, 39, 63 and 64 in

Fig. 1a) were analysed assuming an autosomal recessive mode of inheritance for the SCID disease. The predicted maximum LOD score from this analysis was ~1.9 (that is, $-\log_{10}[0.25 \times 0.25 \times 0.25 \times 0.75]$). For the 'dominant' model, 12 family members with reduced store-operated Ca^{2+} entry were defined as 'affected' (individuals 31, 32, 34, 35, 36, 37, 41, 51, 53, 56, 57 and 63 in Fig. 1a)—that is, carriers of a dominantly acting mutation—and their SNP haplotypes were compared to those of eight healthy family members with normal store-operated Ca^{2+} entry. The predicted maximum LOD score from this analysis was ~3.6 (that is, $-\log_{10}[0.5^{12}]$).

1. Lewis, R. S. Calcium signaling mechanisms in T lymphocytes. *Annu. Rev. Immunol.* **19**, 497–521 (2001).
2. Feske, S., Okamura, H., Hogan, P. G. & Rao, A. Ca^{2+}/calcineurin signalling in cells of the immune system. *Biochem. Biophys. Res. Commun.* **311**, 1117–1132 (2003).
3. Hogan, P. G., Chen, L., Nardone, J. & Rao, A. Transcriptional regulation by calcium, calcineurin, and NFAT. *Genes Dev.* **17**, 2205–2232 (2003).
4. Gallo, E. M., Cante-Barrett, K. & Crabtree, G. R. Lymphocyte calcium signaling from membrane to nucleus. *Nature Immunol.* **7**, 25–32 (2006).
5. Hoth, M. & Penner, R. Depletion of intracellular calcium stores activates a calcium current in mast cells. *Nature* **355**, 353–356 (1992).
6. Zweifach, A. & Lewis, R. S. Mitogen-regulated Ca^{2+} current of T lymphocytes is activated by depletion of intracellular Ca^{2+} stores. *Proc. Natl Acad. Sci. USA* **90**, 6295–6299 (1993).
7. Parekh, A. B. & Putney, J. W. Jr. Store-operated calcium channels. *Physiol. Rev.* **85**, 757–810 (2005).
8. Prakriya, M. & Lewis, R. S. CRAC channels: activation, permeation, and the search for a molecular identity. *Cell Calcium* **33**, 311–321 (2003).
9. Feske, S., Prakriya, M., Rao, A. & Lewis, R. S. A severe defect in CRAC Ca^{2+} channel activation and altered K^+ channel gating in T cells from immunodeficient patients. *J. Exp. Med.* **202**, 651–662 (2005).
10. Partiseti, M. *et al.* The calcium current activated by T cell receptor and store depletion in human lymphocytes is absent in a primary immunodeficiency. *J. Biol. Chem.* **269**, 32327–32335 (1994).
11. Schlesier, M. *et al.* Primary severe immunodeficiency due to impaired signal transduction in T cells. *Immunodeficiency* **4**, 133–136 (1993).
12. Feske, S. *et al.* Severe combined immunodeficiency due to defective binding of the nuclear factor of activated T cells in T lymphocytes of two male siblings. *Eur. J. Immunol.* **26**, 2119–2126 (1996).
13. Feske, S., Giltnane, J., Dolmetsch, R., Staudt, L. & Rao, A. Gene regulation by calcium influx in T lymphocytes. *Nature Immunol.* **2**, 316–324 (2001).
14. Feske, S., Draeger, R., Peter, H. H., Eichmann, K. & Rao, A. The duration of nuclear residence of NFAT determines the pattern of cytokine expression in human SCID T cells. *J. Immunol.* **165**, 297–305 (2000).
15. Feske, S., Draeger, R., Peter, H. H. & Rao, A. Impaired NFAT regulation and its role in a severe combined immunodeficiency. *Immunobiology* **202**, 134–150 (2000).
16. Prakriya, M. & Lewis, R. S. Separation and characterization of currents through store-operated CRAC channels and Mg^{2+}-inhibited cation (MIC) channels. *J. Gen. Physiol.* **119**, 487–507 (2002).
17. Mori, Y. *et al.* Transient receptor potential 1 regulates capacitative Ca^{2+} entry and Ca^{2+} release from endoplasmic reticulum in B lymphocytes. *J. Exp. Med.* **195**, 673–681 (2002).
18. Philipp, S. *et al.* TRPC3 mediates T-cell receptor-dependent calcium entry in human T-lymphocytes. *J. Biol. Chem.* **278**, 26629–26638 (2003).
19. Cui, J., Bian, J. S., Kagan, A. & McDonald, T. V. CaT1 contributes to the stores-operated calcium current in Jurkat T-lymphocytes. *J. Biol. Chem.* **277**, 47175–47183 (2002).
20. Yue, L., Peng, J. B., Hediger, M. A. & Clapham, D. E. CaT1 manifests the pore properties of the calcium-release-activated calcium channel. *Nature* **410**, 705–709 (2001).
21. Voets, T. *et al.* CaT1 and the calcium release-activated calcium channel manifest distinct pore properties. *J. Biol. Chem.* **276**, 47767–47770 (2001).
22. Clapham, D. E. TRP channels as cellular sensors. *Nature* **426**, 517–524 (2003).
23. Putney, J. W. Jr. Capacitative calcium entry: sensing the calcium stores. *J. Cell Biol.* **169**, 381–382 (2005).
24. Roos, J. *et al.* STIM1, an essential and conserved component of store-operated Ca^{2+} channel function. *J. Cell Biol.* **169**, 435–445 (2005).
25. Zhang, S. L. *et al.* STIM1 is a Ca^{2+} sensor that activates CRAC channels and migrates from the Ca^{2+} store to the plasma membrane. *Nature* **437**, 902–905 (2005).
26. Liou, J. *et al.* STIM is a Ca^{2+} sensor essential for Ca^{2+}-store-depletion-triggered Ca^{2+} influx. *Curr. Biol.* **15**, 1235–1241 (2005).
27. Armknecht, S. *et al.* High-throughput RNA interference screens in *Drosophila* tissue culture cells. *Methods Enzymol.* **392**, 55–73 (2005).
28. Boutros, M. *et al.* Genome-wide RNAi analysis of growth and viability in *Drosophila* cells. *Science* **303**, 832–835 (2004).

29. Gwack, Y. et al. A genome-wide Drosophila RNAi screen identifies DYRK as a novel regulator of NFAT. Nature advance online publication, doi:10.1038/nature04631 (1 March 2006).

30. Yeromin, A. V., Roos, J., Stauderman, K. A. & Cahalan, M. D. A store-operated calcium channel in Drosophila S2 cells. J. Gen. Physiol. 123, 167–182 (2004).

31. Homer. The Iliad (Book 5, line 859; Book 8, line 449) (Viking, New York, 1990).

32. Stewart, M. "The Hours", Greek Mythology: From the Iliad to the Fall of the Last Tyrant. http://messagenet.com/myths/bios/hours.html (2005).

33. Altshuler, D. et al. A haplotype map of the human genome. Nature 437, 1299–1320 (2005).

34. Kyte, J. & Doolittle, R. F. A simple method for displaying the hydropathic character of a protein. J. Mol. Biol. 157, 105–132 (1982).

35. Prakriya, M. & Lewis, R. S. Potentiation and inhibition of Ca^{2+} release-activated Ca^{2+} channels by 2-aminoethyldiphenyl borate (2-APB) occurs independently of IP_3 receptors. J. Physiol. (Lond.) 536, 3–19 (2001).

36. Hermosura, M. C., Monteilh-Zoller, M. K., Scharenberg, A. M., Penner, R. & Fleig, A. Dissociation of the store-operated calcium current I_{CRAC} and the Mg-nucleotide-regulated metal ion current MagNuM. J. Physiol. (Lond.) 539, 445–458 (2002).

37. Lepple-Wienhues, A. & Cahalan, M. D. Conductance and permeation of monovalent cations through depletion-activated Ca^{2+} channels I_{CRAC} in Jurkat T cells. Biophys. J. 71, 787–794 (1996).

38. Zweifach, A. & Lewis, R. S. Rapid inactivation of depletion-activated calcium current I_{CRAC} due to local calcium feedback. J. Gen. Physiol. 105, 209–226 (1995).

39. Le Deist, F. et al. A primary T-cell immunodeficiency associated with defective transmembrane calcium influx. Blood 85, 1053–1062 (1995).

40. Doffinger, R. et al. X-linked anhidrotic ectodermal dysplasia with immunodeficiency is caused by impaired NF-κB signaling. Nature Genet. 27, 277–285 (2001).

41. Courtois, G. et al. A hypermorphic IκBα mutation is associated with autosomal dominant anhidrotic ectodermal dysplasia and T cell immunodeficiency. J. Clin. Invest. 112, 1108–1115 (2003).

42. Schmidt-Ullrich, R. et al. Requirement of NF-κB/Rel for the development of hair follicles and other epidermal appendices. Development 128, 3843–3853 (2001).

43. Smahi, A. et al. The NF-κB signalling pathway in human diseases: from incontinentia pigmenti to ectodermal dysplasias and immune-deficiency syndromes. Hum. Mol. Genet. 11, 2371–2375 (2002).

44. Kanno, T. & Siebenlist, U. Activation of nuclear factor-kappaB via T cell receptor requires a Raf kinase and Ca^{2+} influx. Functional synergy between Raf and calcineurin. J. Immunol. 157, 5277–5283 (1996).

45. Crabtree, G. R. & Olson, E. N. NFAT signaling: Choreographing the social lives of cells. Cell 109, S67–S79 (2002).

46. Leykin, I. et al. Comparative linkage analysis and visualization of high-density oligonucleotide SNP array data. BMC Genet. 6, 7 (2005).

47. Gudbjartsson, D. F., Jonasson, K., Frigge, M. L. & Kong, A. Allegro, a new computer program for multipoint linkage analysis. Nature Genet. 25, 12–13 (2000).

Author Contributions S.F. was responsible for all experiments involving genetic and functional analysis of SCID patients, and was assisted in these experiments by S.-H.P. Y.G. designed and implemented the genome-wide Drosophila RNA screen that identified dOrai, with assistance from S.S. M.P. and R.S.L. analysed the electrophysiological properties of calcium currents in Orai1-reconstituted SCID T cells provided by S.F. M.D. advised on the design of the linkage mapping screen and analysis of linkage data, which was carried out by B.T. P.H. and A.R. provided advice and overall direction, and supervised project planning and execution.

Author Information Reprints and permissions information is available at npg.nature.com/reprintsandpermissions. The authors declare no competing financial interests. Correspondence and requests for materials should be addressed to A.R. (arao@cbr.med.harvard.edu).